Mass-Produced, Dispenser-Printed Single-Electrode Triboelectric Nanogenerators for Wearable Applications: A Simple Approach

Chenhao Cong[1,2,†] Fuhao Jiang[1,†], Guangwei Wang[1,†], Hongjiang Li[1], Haoran Zhang[1], Binxuan Diao[1], Enhao Zhao[1], Sang Woo Joo[3,*], Se Hyun Kim[2,*], Xinlin Li[1,*]

[1]College of Mechanical and Electrical Engineering, Qingdao University, Qingdao, 266071, China

[2]School of Chemical Engineering, Konkuk University, Seoul, 05029, Republic of Korea

[3]School of Mechanical Engineering, Yeungnam University, Gyeongsan, Korea 38541, Republic of Korea

Corresponding Author:

*E-mails: swjoo@yu.ac.kr (Sang Woo Joo), shkim97@konkuk.ac.kr (Se Hyun Kim), xinlin0618@163.com (Xinlin Li).

†These authors contributed equally to this work

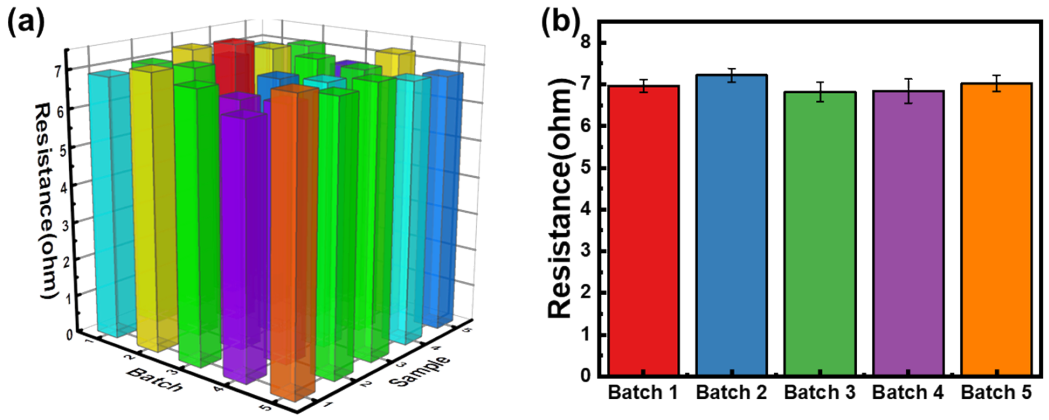

Fig.S1. (a) Electrode properties of different samples in different batches and (b) Electrode properties of different batches.

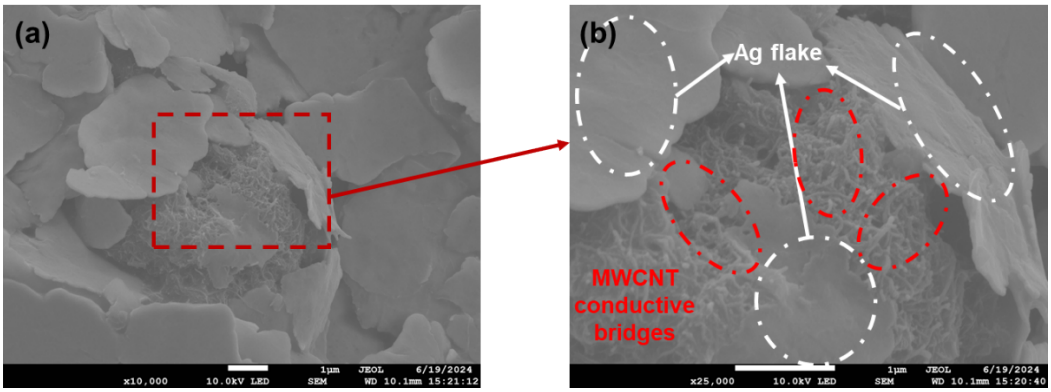

Fig.S2. (a) SEM image of Ag/MWCNT composite and (b) its local enlargement.

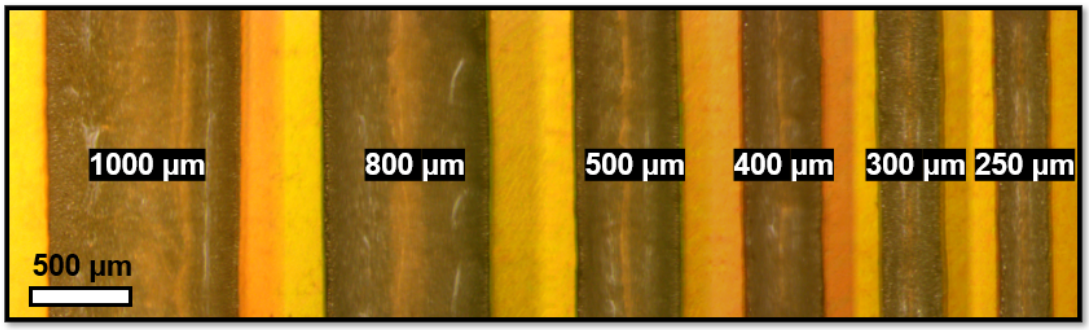

Fig.S3. OM images of differently printed electrodes via dispenser printing parameters.

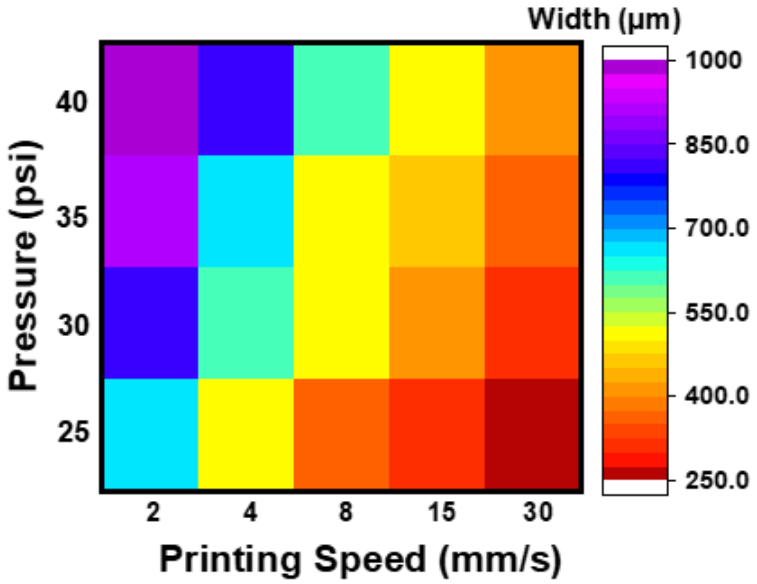

Fig.S4. Flexible electrode measured under OM for various printing parameters against line width.

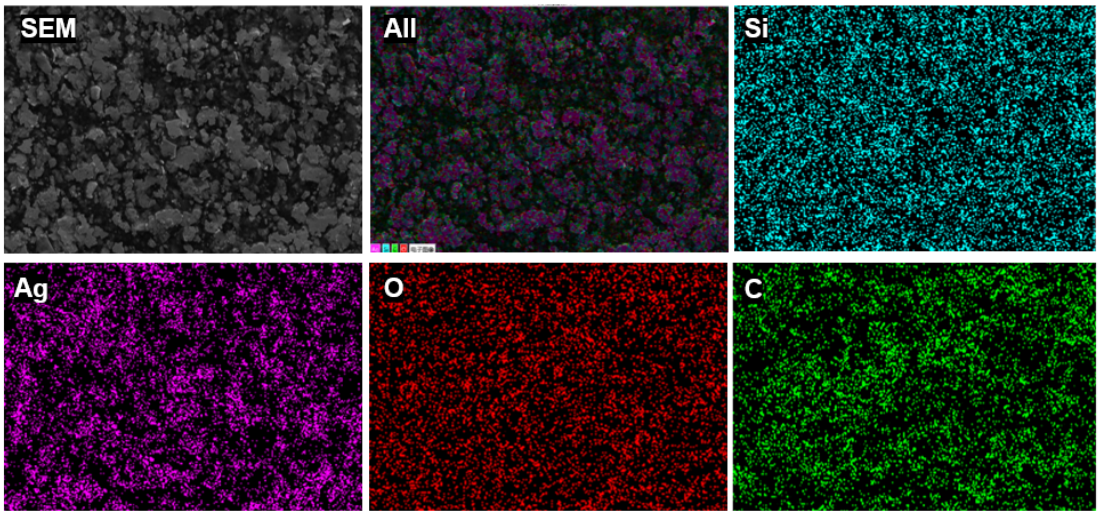

Fig.S5. The SEM images and EDX maps of the Ag/MWCNT/PDMS electrode.

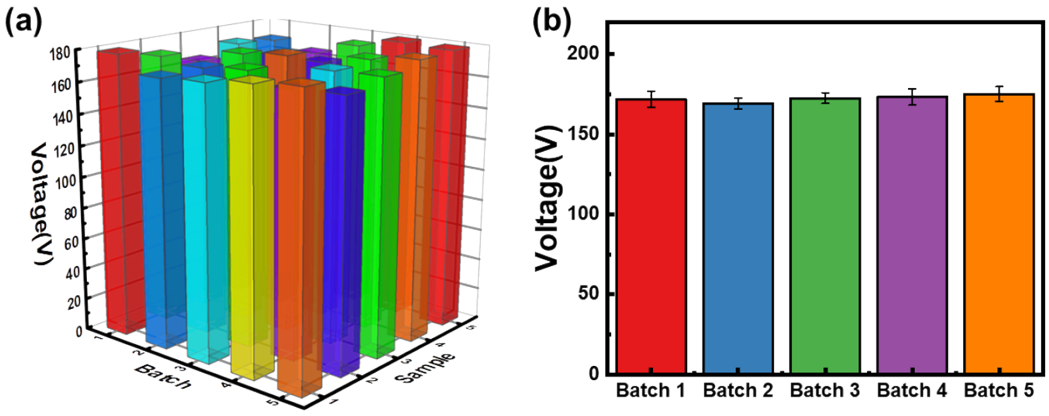

Fig.S6. (a) TENG voltage performance of different batches and samples and (b) Voltage performance of TENG in different batches.

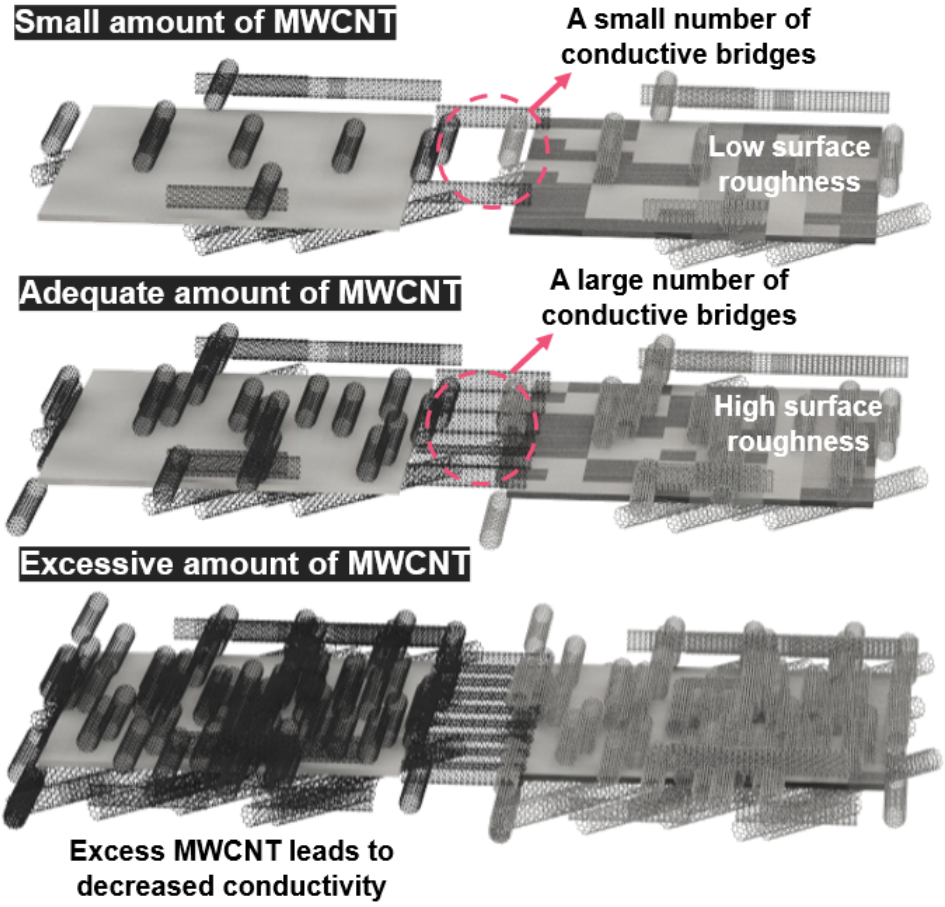

Fig.S7. Schematic representation of the principle of the effect of MWCNT content in the electrode on the performance of TENG.

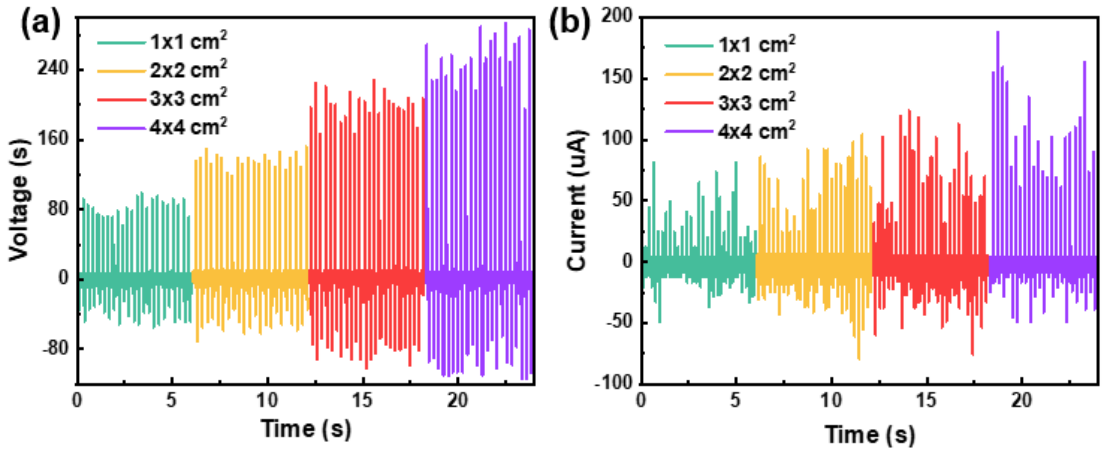

Fig.S8. (a) Open-circuit voltage test and (b) short-circuit current test for devices of different sizes.

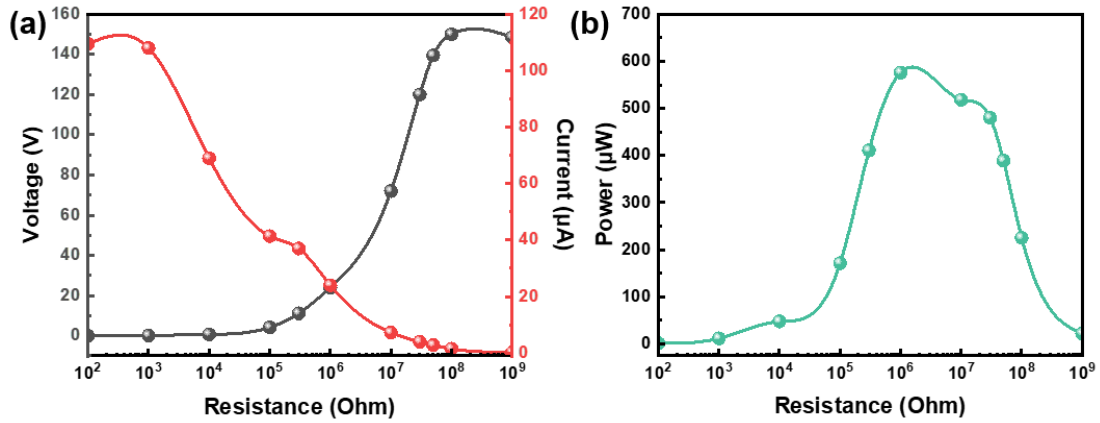

Fig.S9. (a) Load voltage, current and (b) Load power test.

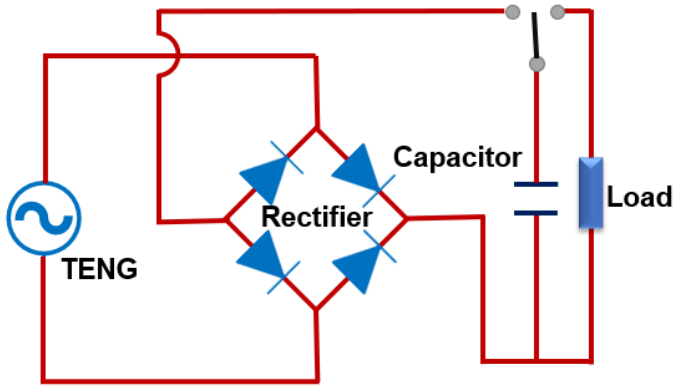

Fig.S10. The working electrical circuit of the TENG-based self-charging system.

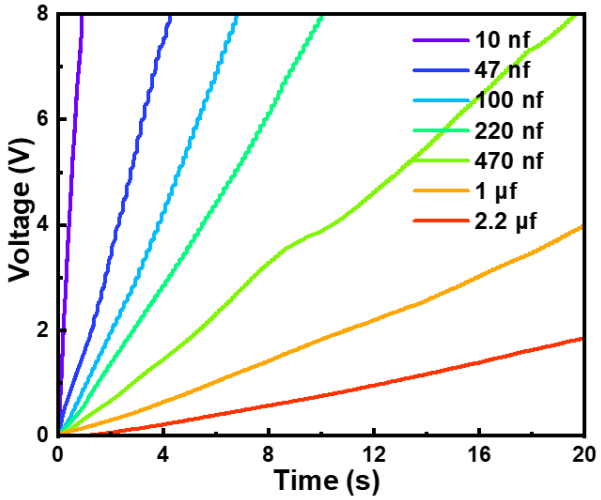

Fig.S11. Charging time diagram of capacitors of different sizes.

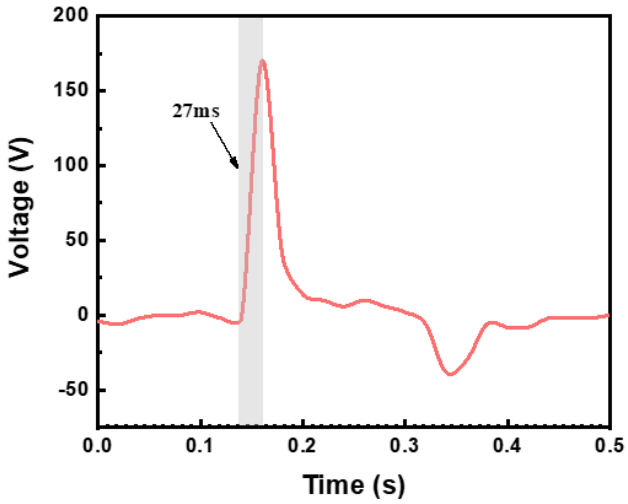

Fig.S12. Response time testing of TENG in human motion detection.

Fig.S13. Physical image of TENG lighting up 30 LED bulbs.

Table.S1 The representative conductive components and properties of negative friction layer materials are reviewed.

Base material	Filler material	Performance		TENG type	Printing type	Ref.
		V_{oc}[V]	I_{sc}[μA]			
PDMS	Ag/MWCNT	172	94	SE	Dispenser printing	This work
Silicone	PEDOT:PSS	8	-	SE	Extrusion printing	[1]
Aluminum foil	ABS	10	0.7	CS	Electrospinning	[2]
PAMPS-PAAm	NaCl	380	5.7	CS	Electrospinning	[3]
PET	PVC	244	6	CS	Electrospinning	[4]
PTFE	NaNbO3	141	3.89	CS	Electrospinning	[5]
PET	Al	125	12.5	CS	Electrospinning	[6]
FEP	Cu	774	3.92	CS	Electrospinning	[7]
PVDF	AgNPs	25	0.22	SE	Screen printing	[6]
Nanopaper	Silver nanoparticles	98.2	13.7	LS	Inkjet printer	[8]
Silicone film	Silver nanoparticles	44.16	-	CS	Direct ink writing	[9]
Bare glass	AgNPs	0.25	1.6e-5	SE	EHD jet printing	[10]

Table.S2 A comparison of the properties of TENG for electrodes of metal and carbon materials is summarized.

Electrode material	Friction layer	Performance		Power	TENG type	Method	Ref.
		V_{oc}[V]	I_{sc}[μA]				
Ag/MWCNT/PDMS	PDMS	172	94	1.45W/m^2	SE	Dispenser printing	This work
rGO/AgNWs	TPU	42	0.1	6mW/m^2	SE	Spraying	[11]
C-AgNW	TPU	12.5	15.8	-	SE	Screen printing	[12]
AgNPs	PVDF	25	0.22	-	SE	Screen printing	[6]
AgNPs	Silicone film	44.16	-	1.03W/m^2	CS	Inkjet printing	[10]
LM/Ag flakes/SEBS	PVDF-HFP	85	8	219.7mW/m^2	SE	Screen printing	[13]
MXene/CNT/PEDOT	PTFE	184.1	4.42	-	CS	Vacuum-assisted filtration	[14]
CNT	Paper	2	0.012	40uW	FT	Inkjet printing	[15]
Graphene/Cu	PDMS	60	14	91.9mW/m^2	SE	Spin-coating	[16]

References

[1] A. Ahmed, I. Hassan, I.M. Mosa, E. Elsanadidy, G.S. Phadke, M.F. El-Kady, J.F. Rusling, P.R. Selvaganapathy, R.B. Kaner, All printable snow-based triboelectric nanogenerator, Nano Energy 60 (2019) 17-25. https://doi.org/10.1016/j.nanoen.2019.03.032.

[2] D. Heo, J. Chung, G. Shin, M. Seok, C. Lee, S. Lee, Yo-Yo Inspired Triboelectric Nanogenerator, Energies 14(7) (2021). https://doi.org/10.3390/en14071798.

[3] B. Ying, R. Zuo, Y. Wan, X. Liu, An Ionic Hydrogel-Based Antifreezing Triboelectric Nanogenerator, ACS Applied Electronic Materials 4(4) (2022) 1930-1938. https://doi.org/10.1021/acsaelm.2c00118.

[4] Y. Chi, K. Xia, Z. Zhu, J. Fu, H. Zhang, C. Du, Z. Xu, Rice paper-based biodegradable triboelectric nanogenerator, Microelectronic Engineering 216 (2019). https://doi.org/10.1016/j.mee.2019.111059.

[5] H.H. Singh, D. Kumar, N. Khare, Tuning the performance of ferroelectric polymer-based triboelectric nanogenerator, Applied Physics Letters 119(5) (2021).

https://doi.org/10.1063/5.0057640.

[6] R. Cao, J. Wang, S. Zhao, W. Yang, Z. Yuan, Y. Yin, X. Du, N.-W. Li, X. Zhang, X. Li, Z.L. Wang, C. Li, Self-powered nanofiber-based screen-print triboelectric sensors for respiratory monitoring, Nano Research 11(7) (2018) 3771-3779. https://doi.org/10.1007/s12274-017-1951-2.

[7] R. Zhang, M. Hummelgård, J. Örtegren, H. Andersson, M. Olsen, W. Chen, P. Wang, C. Dahlström, A. Eivazi, M. Norgren, Energy Harvesting Using Wastepaper‐Based Triboelectric Nanogenerators, Advanced Engineering Materials 25(11) (2023). https://doi.org/10.1002/adem.202300107.

[8] B. Im, S.-K. Lee, G. Kang, J. Moon, D. Byun, D.-H. Cho, Electrohydrodynamic jet printed silver-grid electrode for transparent raindrop energy-based triboelectric nanogenerator, Nano Energy 95 (2022). https://doi.org/10.1016/j.nanoen.2022.107049.

[9] M.-L. Seol, J.-W. Han, D.-I. Moon, K.J. Yoon, C.S. Hwang, M. Meyyappan, All-printed triboelectric nanogenerator, Nano Energy 44 (2018) 82-88. https://doi.org/10.1016/j.nanoen.2017.11.067.

[10] H. Li, X. Fang, R. Li, B. Liu, H. Tang, X. Ding, Y. Xie, R. Zhou, G. Zhou, Y. Tang, All-printed soft triboelectric nanogenerator for energy harvesting and tactile sensing, Nano Energy 78 (2020). https://doi.org/10.1016/j.nanoen.2020.105288.

[11] K. Zhou, Y. Zhao, X. Sun, Z. Yuan, G. Zheng, K. Dai, L. Mi, C. Pan, C. Liu, C. Shen, Ultra-stretchable triboelectric nanogenerator as high-sensitive and self-powered electronic skins for energy harvesting and tactile sensing, Nano Energy 70 (2020). https://doi.org/10.1016/j.nanoen.2020.104546.

[12] G. Zhu, P. Ren, J. Yang, J. Hu, Z. Dai, H. Chen, Y. Li, Z. Li, Self-powered and multi-mode flexible sensing film with patterned conductive network for wireless monitoring in healthcare, Nano Energy 98 (2022). https://doi.org/10.1016/j.nanoen.2022.107327.

[13] Y. Li, J. Xiong, J. Lv, J. Chen, D. Gao, X. Zhang, P.S. Lee, Mechanically interlocked stretchable nanofibers for multifunctional wearable triboelectric nanogenerator, Nano Energy 78 (2020). https://doi.org/10.1016/j.nanoen.2020.105358.

[14] X. Yang, F. Wu, C. Xu, L. Yang, S. Yin, A flexible high-output triboelectric nanogenerator based on MXene/CNT/PEDOT hybrid film for self-powered wearable sensors, Journal of Alloys and Compounds 928 (2022). https://doi.org/10.1016/j.jallcom.2022.167137.

[15] D.-S. Zhang, W.-Z. Song, L.-X. Wu, C.-L. Li, T. Chen, D.-J. Sun, M. Zhang, T.-T. Zhang, J. Zhang, S. Ramakrishna, Y.-Z. Long, In-plane electrodes enhance the output performance of triboelectric nanogenerators and their applicability in IoT applications, Nano Energy (2023). https://doi.org/10.1016/j.nanoen.2023.108313.

[16] Y. Li, W. Zheng, H. Zhang, H. Wang, H. Cai, Y. Zhang, Z. Yang, Electron transfer mechanism of graphene/Cu heterostructure for improving the stability of triboelectric nanogenerators, Nano Energy 70 (2020). https://doi.org/10.1016/j.nanoen.2020.104540.